Research Journal of Chemical Sciences _____ ISSN 2231-606X
Vol. **5(10),** 51-61, October **(2015)** *Res. J. Chem. Sci.*

Effect of Substrate Temperature on Structural and Optical Properties of Cu_2ZnSnS_4 (CZTS) Films Prepared by Chemical Spray Pyrolysis Method

Nabeel A. Bakr*, Ziad T. Khodair and Shahlaa M. Abdul Hassan
Department of Physics, College of Science, University of Diyala, Diyala, IRAQ

Available online at: www.isca.in, www.isca.me
Received 2nd October 2015, revised 9th October 2015, accepted 17th October 2015

Abstract

In this work Copper zinc tin sulfide (CZTS) films were prepared by using chemical spray pyrolysis technique. Copper chloride CuCl, Zinc chloride $ZnCl_2$, Tin chloride pentahydrate $SnCl_4.5H_2O$ and Thiourea $SC(NH_2)_2$ were used as sources of Copper ions, Zinc ions, Tin ions and Sulfur ions respectively. CZTS thin films have been grown on clean preheated glass at different substrate temperatures of (200, 250, 300, 350, 400 and 450) ^oC. The structural and optical properties of these films have been studied using XRD, AFM, and UV-Visible spectroscopy. The XRD results showed that all films are polycrystalline in nature with tetragonal structure and preferred orientation along (112) plane. The crystallite size was calculated using Scherrer's formula and it is found that the CZTS thin films have maximum crystallite size of (34.401 nm) at substrate temperature of 450 ^oC. Williamson-Hall analysis was carried out for all samples and the crystallite size along with microstrains were estimated. AFM results showed homogenous and smooth thin films. The absorbance and transmittance spectra have been recorded in the wavelength range of (300- 900) nm in order to study the optical properties. The optical energy gap for allowed direct electronic transition was calculated using Tauc's equation. It is found that the band gap decreases as the substrate temperature increases and the optical allowed energy gap for the direct electronic transitions was in the range of (2.3 -1.85) eV. Urbach energy values range between (477 - 643) meV. The optical constants including absorption coefficient, real and imaginary parts of dielectric constant were also calculated as a function of photon energy. Refractive index and extinction coefficient were estimated as a function of wavelength.

Keywords: CZTS thin films, substrate temperature, structural properties, Williamson – Hall analysis, optical properties, AFM.

Introduction

Cu_2ZnSnS_4 (CZTS) is recently considered as one of the most important compound semiconductors due to its applications in thin film solar cells and other optoelectronics devices. CZTS is a direct band gap material having energy gap values located within the solar radiation spectrum. Moreover, its constituents are inexpensive and do not contain any toxic materials like cadmium and lead[1]. Because of these special properties, this material is currently of high interest in the field of manufacturing cheap, non-toxic and efficient solar cells[2-4]. Chemical spray pyrolysis technique has attracted many research groups to prepare different types of thin film materials because it is considered as a low-cost technique comparing with other methods which usually require high-cost devices and complex instrumentation such as vacuum systems. Furthermore, it does not require high quality targets or substrates and can be easily scaled up for industrial applications[5,6]. In the current study, the structural and optical properties of CZTS thin films deposited by chemical spray pyrolysis technique at different substrate temperatures are reported.

Material and Methods

Cu_2ZnSnS_4 thin films were deposited by spray pyrolysis technique. The precursor solution was obtained by mixing aqueous solutions of 0.04 mol/L of CuCl, 0.02 mol/L of $ZnCl_2$, 0.02 mol/L of $SnCl_4.5(H_2O)$ and 0.16 mol/L of $SC(NH_2)_2$ with a final volume of 100 mL. The ratio of elements Cu/Zn/Sn/S in the precursor solution was 2/1/1/8.

Experiments were conducted at various substrate temperatures in the range of (200–450)^oC to investigate the effect of substrate temperature on the growth of the films keeping the other parameters constant. The resultant solution was sprayed on glass substrates. Other deposition conditions such as spray nozzle substrate distance (30 cm), spray time (10 s), spray interval (2 min) and pressure of the carrier gas (1.5 bar) were kept constant for each concentration.

The thickness of deposited films was about 400±10 nm measured by the conventional gravimetric technique. The X-ray diffraction patterns for the prepared films were obtained in a (Shimadzu XRD-6000) goniometer using copper target (CuKα, 1.5418 Å) and Atomic Force Microscopy (AFM) micrographs were recorded by using scanning probe microscope type (SPM-AA3000), contact mode, supplied by Angstrom Advanced Inc. Optical properties in the wavelength range of (300 - 900) nm were investigated by using UV-VIS-NIR spectroscopy (Shimadzu, UV-1800).

Results and Discussion

Structural analysis: XRD patterns of the CZTS films are shown in figure-1. It can be noticed that all the patterns exhibit diffraction peaks around (2θ~28°, 32°, 47° and 56°) referred to (112), (200), (220) and (312) favorite directions respectively which is in agreement with the International Center of Diffraction Data (ICDD) card number 26-0575. The strongest peak occurs at 2θ~28° which is referred to (112) plane. The positions of the peaks and the presence of more than one diffraction peak lead to the conclusion that the films are polycrystalline in nature with a tetragonal crystalline structure, which is in agreement with other reports[7-9].

It can be noticed that 2θ position for (112) direction shifts to higher values as substrate temperature increases from 200 °C to 400 °C, whereas at substrate temperature of 450 °C the 2θ shifts back to a lower value as shown in table-1. The full width at half maximum (FWHM) of preferential orientation shows that it has a decreasing trend as temperature increases. The lattice parameter was found to vary from a = 0.5380 nm to 0.5415 nm and from c = 1.0693 nm to 1.0873 nm. These values are in agreement with theoretical values a = 0.542 nm and c = 1.0848 nm[10,11]. In Tetragonal ideal structure, the ratio of the lattice vector (c/a) is 2. In the present work two cases are noticed. First, the ratio is less than 2, which implies that the lattice is compressed in the c-axis direction, and second, the ratio is greater than 2, indicating that the lattice is elongated along the c-axis. It is important to mention here that there is a very low intensity peak at 2θ ≈ 46° which does not belong to the standard CZTS phase. This peak is assigned by (♦) in figure-1. This diffraction peak may be attributed to Cu_xS phase as reported by previous studies[12]. The possible reason behind the appearance of this secondary phase is the high concentration of thiourea in the sprayed solution. When the concentration of sulphur, which is electronegative element, increases in the starting solution, it may instantaneously react with metal ions available to form secondary phases[13].

The average crystallite size and microstrains induced in the films can be determined using Williamson-Hall (W- H) formula shown below[14]:

$$\boldsymbol{\beta_{hkl}\cos\theta = (K\lambda/D_{av}) + 4S\sin\theta} \quad (1)$$

Where β_{hkl} is full width of half maximum, D_{av} is the average crystallite size, k is constant and was assumed to be equal to 0.9, λ is wavelength for Cu target for XRD instrument, θ is Bragg's angle for all peaks, and S is the microstrain in the film. If βcosθ is plotted with respect to 4sinθ for all peaks, microstrain and crystallite size can be calculated from the slope and y-intercept of the fitted line respectively as shown in Figure-2. The average crystallite size for the all films is also calculated for (112) direction by Scherrer's formula by using the relation[15]:

$$D_{av} = \frac{K\lambda}{\beta\cos\theta} \quad (2)$$

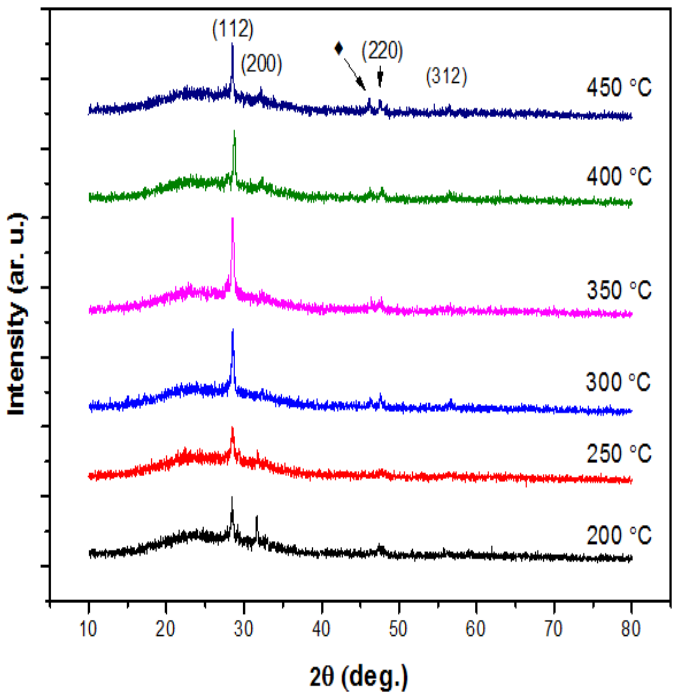

Figure-1
X-Ray diffraction patterns of the CZTS thin films

It is observed that the average crystallite size has an increasing trend as substrate temperature increases as shown in Figure-3 and this result is in agreement with previous studies which indicates the crystal structure improvement with substrate temperature[12,16,17]. It is reported that when the substrate temperature increases, the mobility of the atoms located on the surface increases, so these atoms can rearrange their positions to occupy more stable sites. This process controls the favorite growth orientation of the crystal structure. All values of microstrain were negative which indicates the occurrence of compression in the lattice, as shown in Table-1. The microstrains are induced during the growth of thin films, and will be raised from stretching or compression in the lattice[18].

The texture coefficient (Tc) represents the texture of a particular plane, in which greater than unity values imply that there are numerous of grains in that particular direction. The texture coefficients Tc(*hkl*) for all samples have been calculated from the X-ray data using the well-known formula[19]:

$$\mathbf{T_c(hkl)} = \frac{\mathbf{I(hkl)/I_o(hkl)}}{\mathbf{N_r^{-1}\sum I(hkl)/I_o(hkl)}} \quad (3)$$

Where I(hk*l*) is the measured intensity, I_o(hk*l*) taken from the (ICDD), (N_r) is the number of reflections and (hk*l*) is Miller indices. The texture coefficient is calculated for crystal plane (112) of the CZTS thin films. The texture coefficient T_c values are (>1) for all films indicating that there are numerous grains in the (112) favorite direction.

AFM Results: The 3D AFM micrographs of CZTS thin films are shown in figure-4. The size of the scanned area was (2x2) μm^2. The grain size, average roughness and root mean square roughness of the film at different substrate temperatures are shown in table-2. It is clear that the grain size varies randomly, from one zone to another, between 87.00 and 104.39 nm, which is in agreement with the result recorded by Kamoun et al.[17]. When comparing these values with the crystallite size obtained by XRD, it can be inferred that most grains observed in AFM are aggregates of smaller crystallites. On the other hand, from the same table the root mean square and surface roughness vary in contrast manner with substrate temperature.

Table-1
Structural parameters of CZTS thin films

Substrate Temperature T_S (^oC)		200	250	300	350	400	450
2Θ (deg)		28.5003	28.5333	28.5649	28.5742	28.7752	28.5425
hkl		(112)	(112)	(112)	(112)	(112)	(112)
d (Å)		3.12932	3.12577	3.12239	3.12139	3.10005	3.12479
(FWHM) (rad)		0.0680	0.0739	0.0545	0.0638	0.0484	0.0415
(D_{av}) nm Scherrer		21.03	19.5	26.22	22.40	29.54	34.40
(D_{av}) nm W-H		20.06	14.50	21.13	20.2	26.1	32.3
Microstrain S		- 0.0012	- 0.0035	- 0.0014	- 0.0015	- 4.4436	- 1.4806
Lattice Constants (nm)	a	0.5415	0.5444	0.5402	0.5405	0.5380	0.5405
	c	1.0860	1.0709	1.0839	1.0816	1.0693	1.0850
(c/a)		2.005	2.012	2.006	2.001	1.987	2.007
T_c		1.107	1.222	1.654	1.853	1.192	1.074

Table-2
Surface roughness, root mean square and grain size of CZTS thin films

Temperature substrate T_S (^oC)	**Surface roughness (nm)**	**RMS (nm)**	**Grain size (nm)**
200	8.26	9.49	104.39
250	6.39	7.33	91.82
300	23.9	27.4	87.00
350	23.8	27	91.46
400	11.5	13.3	94.65
450	4.84	5.61	94.36

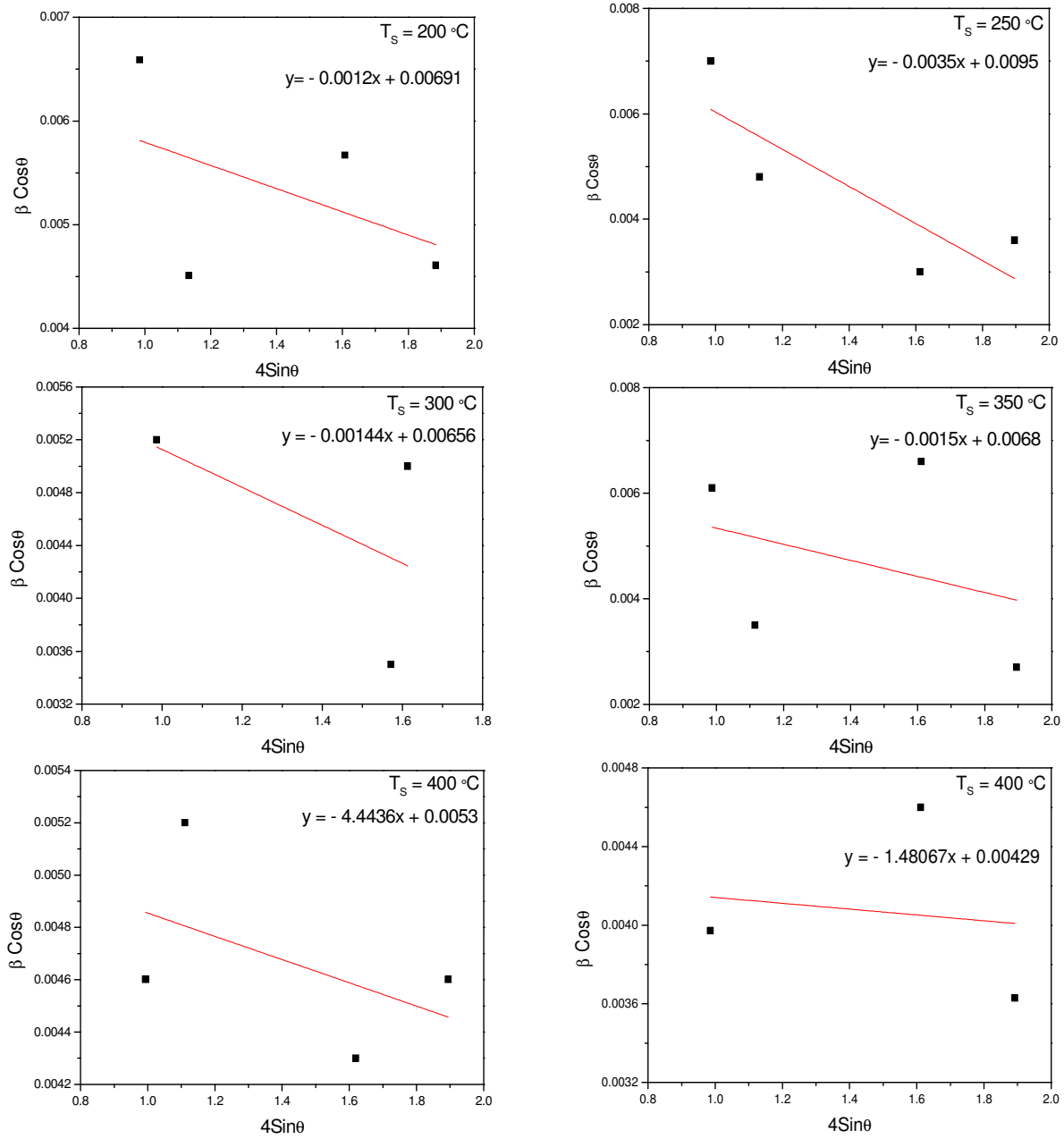

Figure-2
W-H analysis for CZTS thin films deposited in the present study

Optical analysis: Optical absorption spectra of the films in spectral range of (300 – 900) nm were recorded by using UV–visible spectrophotometer. The analysis of the dependence of absorption coefficient on photon energy in the high absorption regions is performed to obtain the detailed information about the energy band gaps of the films. Figure-5 shows the relation between transmittance and wavelength for CZTS thin films.

It can be noticed that the transmittance increases rapidly as the wavelength increases in the range of (367- 600 nm), and then increases slowly at higher wavelengths.

The films have high transparency in the visible and near IR regions of the electromagnetic spectrum with transmittance value of about (80 %) recorded at (λ > 800 nm) with substrate temperature 200 ^{o}C , therefore more attention has been paid to study this type of films for using in solar cells. The transmittance decreases with elevating the substrate temperature which is in agreement with other studies[20,21]

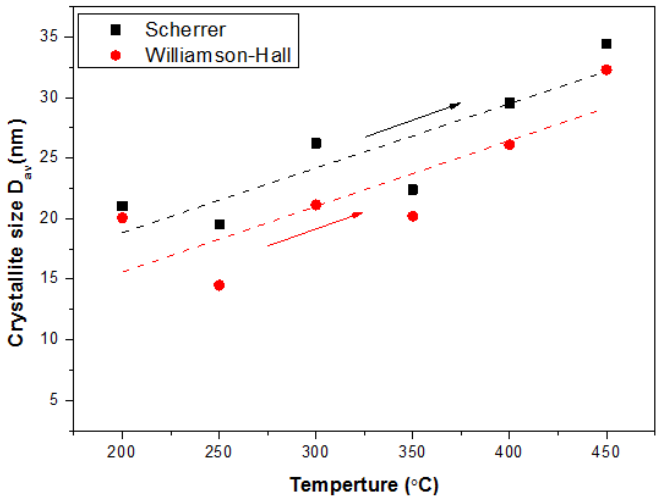

Figur-3
Crystallite size of CZTS thin films estimated by Sherrer's formula and Williamson-Hall analysis

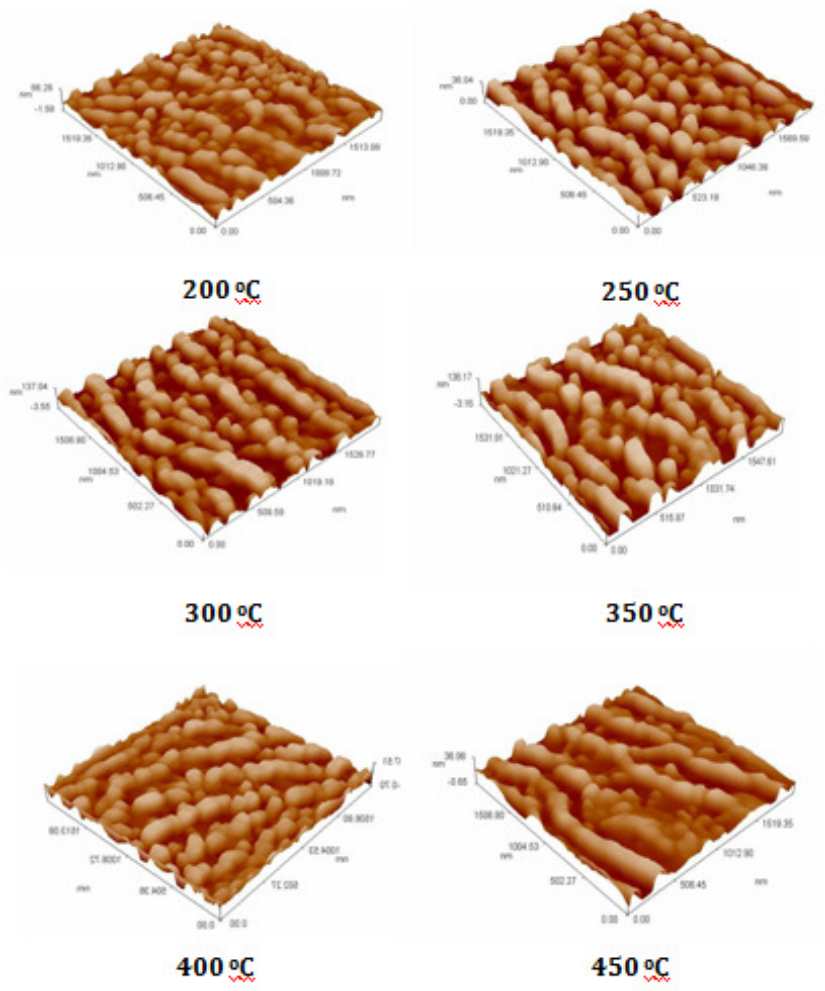

Figure-4
3D AFM images of CZTS deposited films

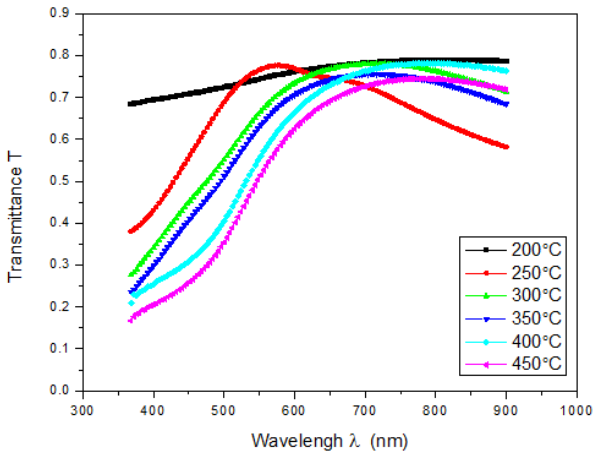

Figure-5
Transmittance (T) versus wavelength (λ) for CZTS thin films.

Figure-6 shows the relation between absorbance (A) and wavelength for the deposited thin films. The absorbance decreases rapidly at short wavelengths corresponding to the energy gap of the film. This evident increase of energy is due to the interaction of the material electrons with the incident photons which have enough energy for the occurrence of electron transitions. It is observed that the absorbance increases as the substrate temperature increases in agreement with other reports[22,23].

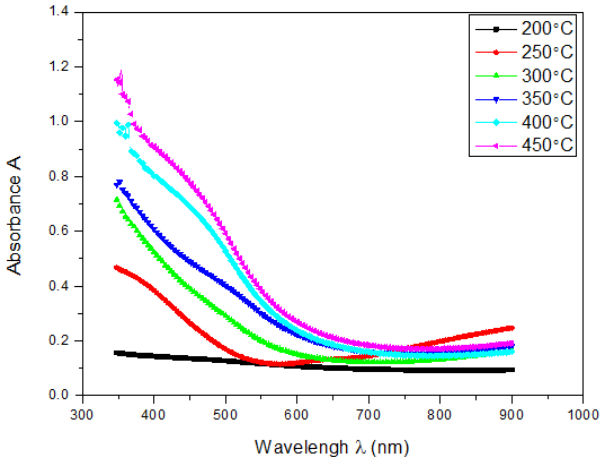

Figure-6
Absorbance (A) versus wavelength (λ) for CZTS thin films

The absorption coefficient is estimated from the absorbance using the well-known formula[24]:

$$\alpha = (2.303 \times A)/t \quad (4)$$

Where A is the absorbance, t is the thickness and α is the absorption coefficient. Figure-7 shows the optical absorption coefficient as a function of photon energy on CZTS thin films at different substrate temperatures. It can be seen that CZTS thin film has a value of absorption coefficient $\alpha > 10^4$ cm^{-1} which indicates the increase of the probability of the occurrence of direct transitions. It have been noticed that all the prepared thin films have high absorption coefficient between 10^4 and 10^5 cm^{-1} in visible range and the near-IR spectral range which is in agreement with other reports[11]. It can be noticed also that the absorption coefficient increases with increasing substrate temperature.

The optical energy band gap (E_g) is given by the classical relation[25]:

$$\alpha h\nu = A\,(h\nu - E_g)^r \quad (5)$$

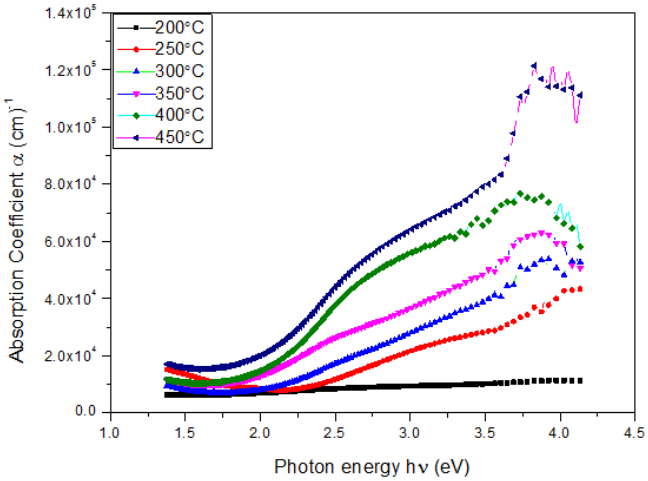

Figure-7
Absorption coefficient versus photon energy for CZTS thin films

Where α is the absorption coefficient, hν is the photon energy, E_g is the optical band gap, A is a constant which does not depend on photon energy and r has four numeric values (1/2) for allowed direct, 2 for allowed indirect, 3 for forbidden direct and (3/2) for forbidden indirect optical transitions. In this work, direct band gap was determined by Tauc's equation. Plotting a graph between $(\alpha h\nu)^2$ and (hν) in eV, a straight line is obtained. The extrapolation of this straight line to $(\alpha h\nu)^2 = 0$ gives value of the direct band gap of the material[26], and this could be seen in figure-8. It can be observed that the band gap value decreases as the substrate temperature increases, which is in agreement with other reports[27-29] suggesting that the deposited films are good candidates for the absorber layer in solar cells. The obtained E_g values are shown in figure-9.

The region in the absorption spectrum which has an exponential dependence of the absorption coefficient on the photon energy is called Urbach edge which reflects the transitions between the valance and conduction band tail states. The absorption coefficient in this region can be expressed by the following relation[24]:

$$\alpha = \alpha_o \exp(h\nu/E_u) \quad (6)$$

Where E is the photon energy, α_o is constant, and E_u is the Urbach energy. Figure-10 shows the variation of (lnα) energy for the films. The E_u values were calculated as the reciprocal of the straight line slopes shown in the figure. It is observed that the Urbach energy has decreasing trend as the substrate temperature increases. This result supports the improvement of the crystal structure concluded from XRD analysis. The obtained E_u values are plotted in the inset of figure-9. The refractive index has been calculated using the relation[30]:

$$n = \left[\frac{(1+R)^2}{(1-R)^2} - \left(k_o^2 - 1\right)\right]^{1/2} + \frac{(1+R)}{(1-R)} \quad (7)$$

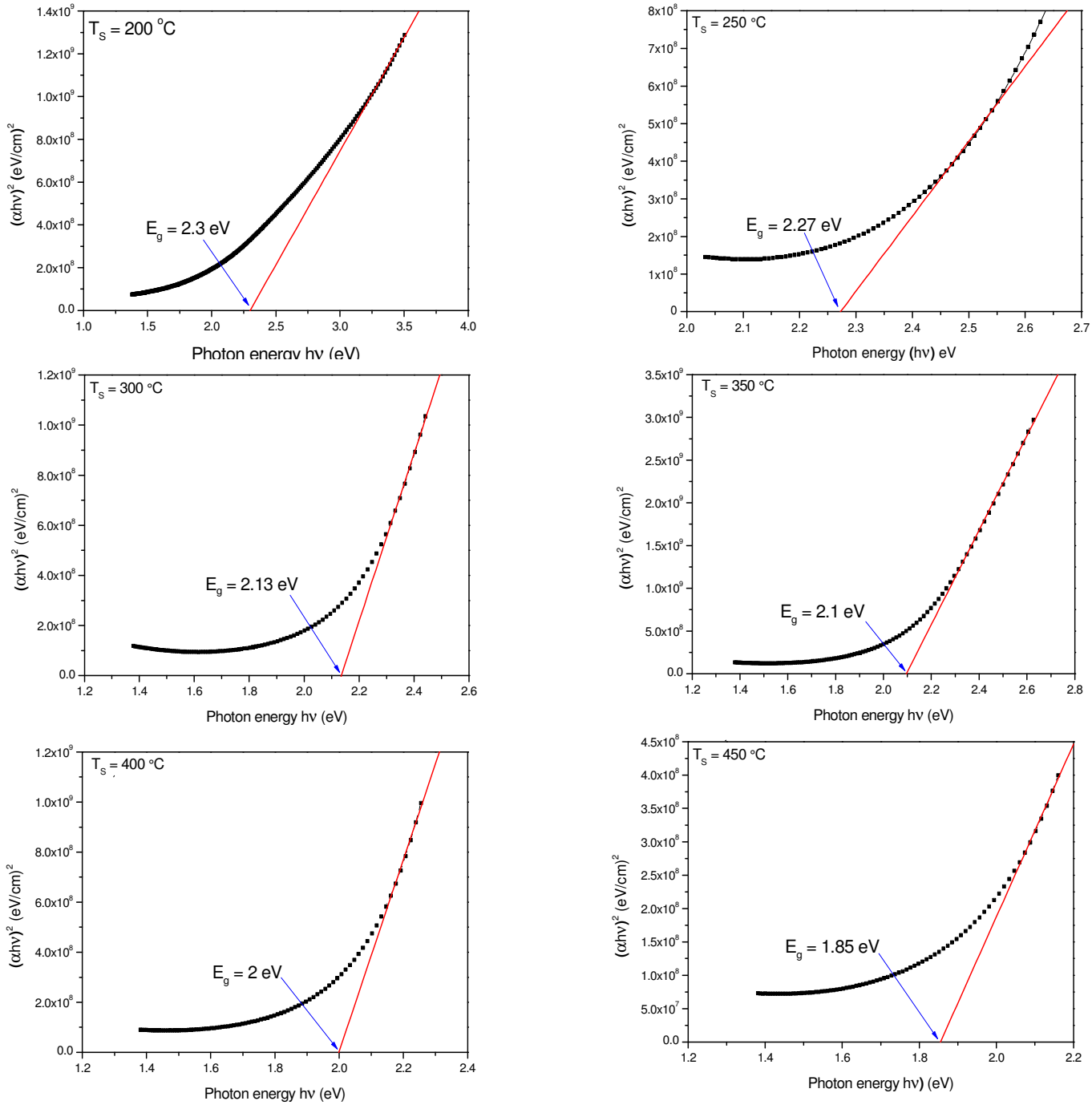

Figure-8
The relation between (α hν)^2 and (hν) for CZTS thin films

Where n is the refractive index, R is the reflectance and K_o is the extinction coefficient. The relation between refractive index and wavelength of incident photon of CZTS thin films at different substrate temperature is shown in Figure-11. It can be seen that the refractive index of the prepared films are in the range of (1.75 - 2.64). It can be observed that the refractive index has an increasing trend with substrate temperature. This increase can be attributed to the film densification and improvement in the crystallinity of the films. This result is in agreement with other reports[15]. The extinction coefficient (K_o) was calculated using relation[31,32]:

$$K_o = \alpha\lambda/4\pi \quad (8)$$

Where K_o is the extinction coefficient and λ is the wavelength of incident photon. The relation between extinction coefficient and wavelength for CZTS thin films is shown in Figure-12. The extinction coefficient (K_o) decreases rapidly at short wavelengths (450-600) nm and after that the values of (K_o) remains almost constant. The rise and fall in the value of (K_o) is directly related to the absorption of light. The lower value of (K_o) in the wavelength range (600-900) nm implies that these films absorb light in this region very easily. Variation in the extinction coefficient values is directly related to the absorption of light. The extinction coefficient of prepared films have values in the range of (0.025 - 0.195).

The dielectric constant can be represented by the following equation[33]:

$$\varepsilon = \varepsilon_1 + i\,\varepsilon_2 \quad (9)$$

Where ε_1 is the real part of the complex dielectric constant and ε_2 is the imaginary part of it. For the calculation of the dielectric constant in its two parts one can use the following expressions[34]:

$$\varepsilon_1 = (n^2 - K_o^2) \quad (10)$$

$$\varepsilon_2 = 2\,n\,K_o \quad (11)$$

The plots of real and imaginary part of all samples were illustrated in figure-13 which shows that ε_1 for all samples behave like the refractive index as a function of λ and ε_2 for all samples behave like the extinction coefficient as a function of λ.

Conclusion

In this study CZTS thin films were successfully deposited on glass substrates by chemical spray pyrolysis technique. XRD patterns of the CZTS thin films indicate that all films are polycrystalline with tetragonal structure. The main characteristic peaks are assigned to the (112), (200), (220) and (312) planes. A very low intensity peak at $2\theta \approx 46^o$ which doesn't belong to the CZTS phase was observed. This diffraction peak was attributed to Cu_xS phase. The possible reason behind the appearance of this secondary phase is the high concentration of thiourea in the sprayed solution. When the concentration of sulphur, which is electronegative element, increases in the starting solution, it may instantaneously react with metal ions available to form secondary phases. It is observed that the average crystallite size has an increasing trend as substrate temperature increases and this result indicates the crystal structure improvement with substrate temperature. AFM results showed homogenous and smooth thin films. When comparing the grain size values obtained from the granularity report of AFM with the crystallite size obtained by XRD, it can be inferred that most grains observed in AFM are aggregates of smaller crystallites. The transmittance of CZTS thin films increases rapidly as the wavelength increases in the range of (367- 600) nm, and then increases slowly at higher wavelengths. The band gap value decreases when the substrate temperature increases suggesting that the deposited films are good candidates as absorber layer in solar cells. The Urbach energy has decreasing trend as the substrate temperature increases. This result supports the improvement of the crystal structure concluded from XRD analysis.

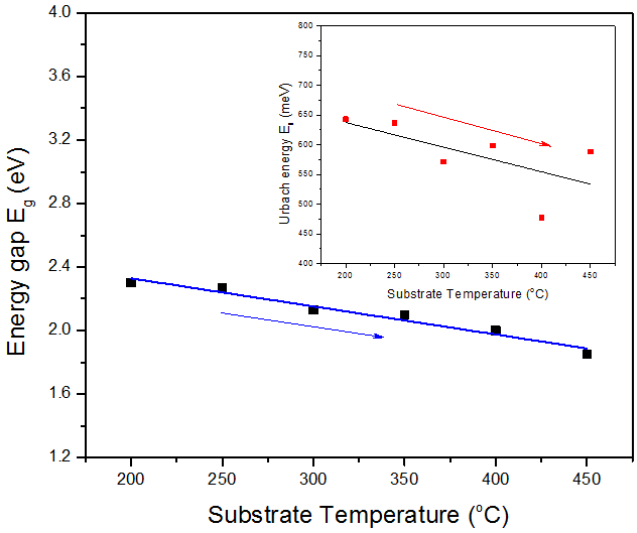

Figure-9
Energy gap and Urbach energy (inset) as a function of substrate temperature of CZTS thin films

References

1. Pandey Bhawana and Fulekar M. H., Nanotechnology: Remediation Technologies to clean up the Environmental pollutants, *Res. J. chem. sci.,* **2(2),** 90-96**(2012)**
2. Mitzi D.B., Gunawan O., Todorov T.K., Wang K. and Guha S., The path towards a high-performance solution-processed kesterite solar cell, *Sol. Energ. Mat. Sol. Cells*, **95(6)**, 1421-1436**(2011)**
3. Siebentritt S. and Schorr S., Kesterites - a challenging material for solar cells, *Prog. Photovoltaics Re. S Appl.*, **20(5)**, 512-519 **(2012)**

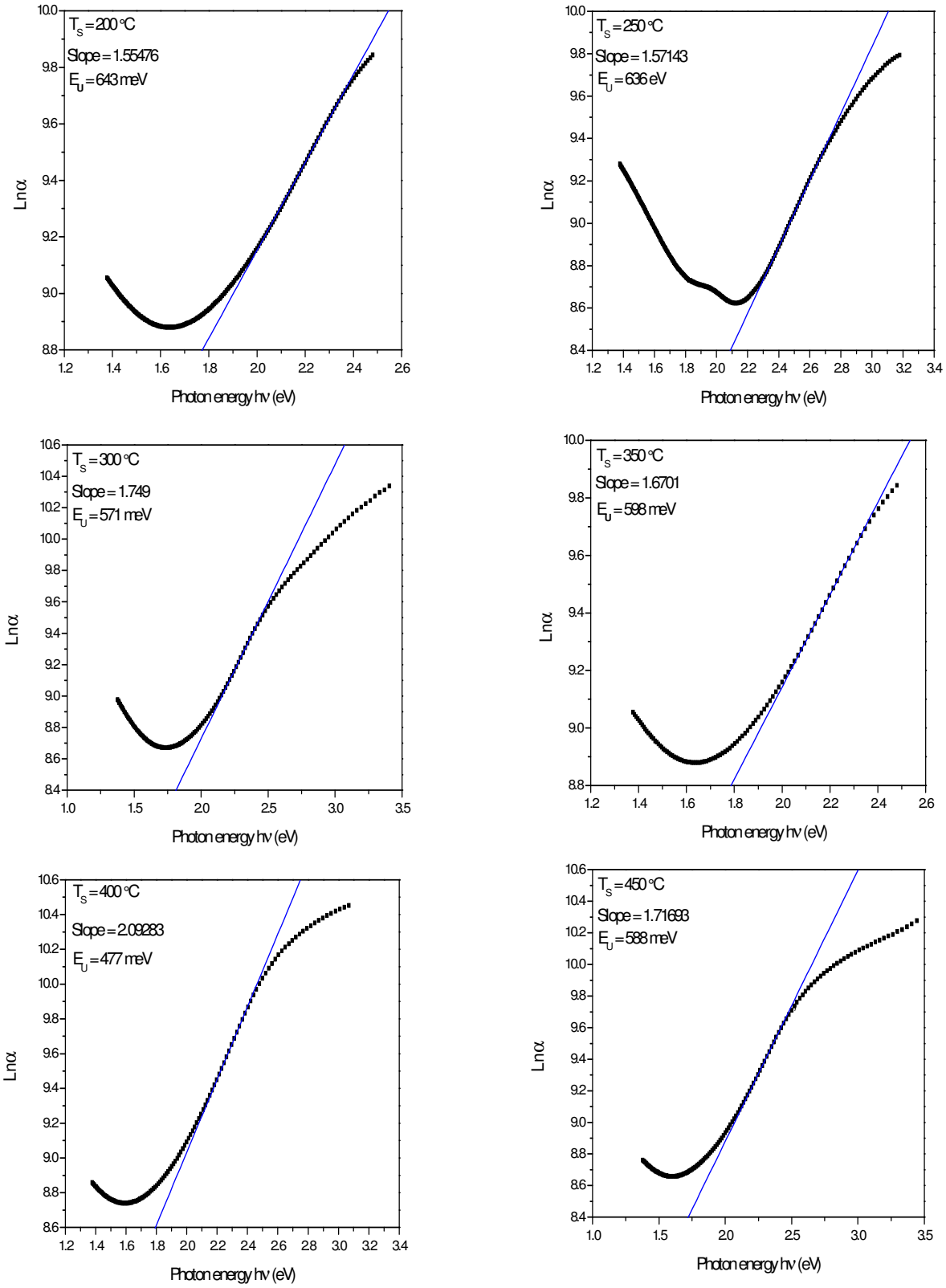

Figure-10
Urbach plots of CZTS thin films

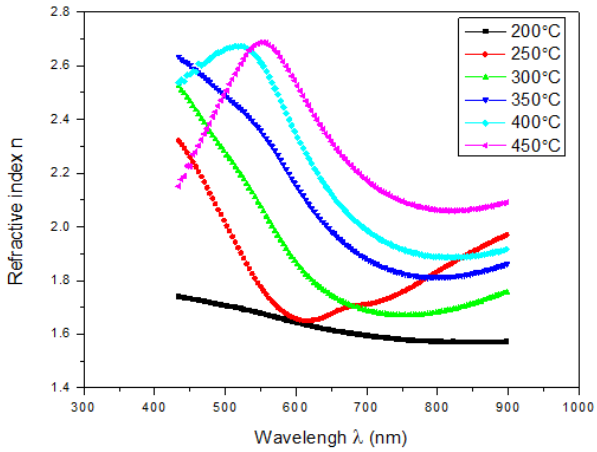

Figure-11
Refractive index versus wavelength of CZTS thin films

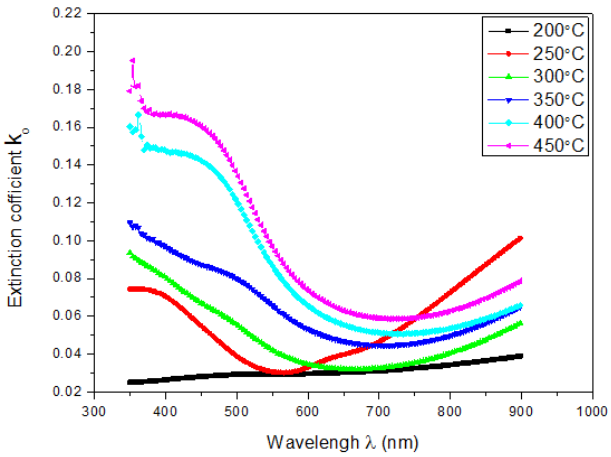

Figure-12
Extinction coefficient versus wavelength of CZTS thin films

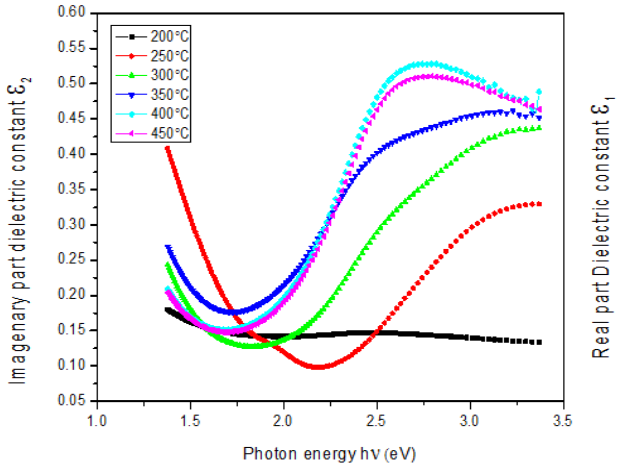

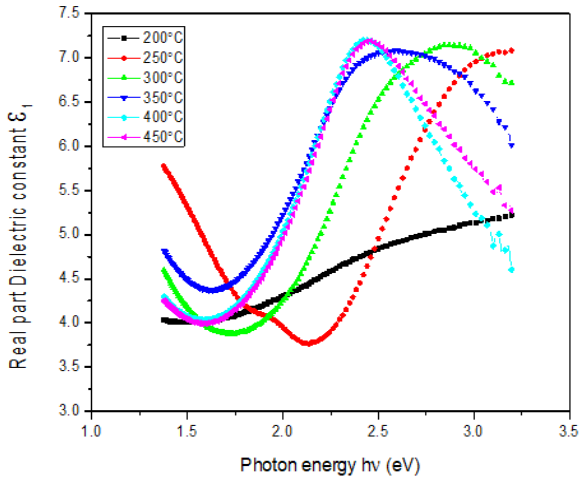

Figure-13
Real and imaginary parts of dielectric constant versus photon energy of CZTS thin films

4. Todorov T.K., Tang J., Bag S., Gunawan O., Gokmen T., Zhu Y. and Mitzi D.B., Beyond 11% efficiency: characteristics of state-of-the-art $Cu_2ZnSn(S,Se)_4$ solar cells, *Adv. Energy Mater.*, **1(3)**, 34–38 **(2013)**

5. Pramod S. Patil, Versatility of chemical spray pyrolysis technique, *Mater. Chem. Phys.*, **59(3)**, 185–198 **(1999)**

6. Nakayama N. and Ito K., Sprayed films of stannite Cu_2ZnSnS_4, *Appl. Surf. Sci.*, **92**, 171–175 **(1996)**

7. Valdes M., Santoro G. and Vazquez M., Spray deposition of Cu_2ZnSnS_4 thin films, *J. Alloy Compd.*, **585**, 776–782 **(2014)**

8. Deokate R.J., Adsool A.D., Shinde N.S., Pawar S.M. and Lokhande C.D., Structural and Optical properties spray-deposited Cu_2ZnSnS_4 thin films, *Energy procedia*, **54**, 627-633 **(2014)**

9. Subramania E.P., Rajesh G., Muthukumarasamy N., Thambidurai M., Asokan V. and Velauthapillai D., Solar cells of Cu_2ZnSnS_4 thin films prepared by chemical bath deposition method, *Indian J. Pure Ap. Phy.*, **52**, 620-624 **(2014)**

10. Kishore Kumar Y.B., Suresh Babu G., Uday Bhaskar P. and Sundara Raja V., Preparation and characterization of spray-deposited Cu_2ZnSnS_4 thin films, *Sol. Energ. Mat. Sol. Cells*, **93(8)**, 1230–1237 **(2009)**

11. Sheleg A.U., Hurtavy V.G., Mudryi A.V., Valakh M. Ya., Yukhymchuk V.O., Babichuk I.S., Leon M. and Caballero R., Determination of the Structural and Optical Characteristics of Cu_2ZnSnS_4 Semiconductor Thin Films, *Semiconductors*, **48(10)**, 1296–1302 **(2014)**

12. Touati R., Ben Rabeh M. and Kanzari M., Effect of post-sulfurization on the structural and optical properties of Cu_2ZnSnS_4 thin films deposited by vacuum evaporation method, *Thin Solid Films*, **582**, 198-202 **(2015)**

13. Kishore Kumar Y.B., Uday Bhaskar P., Suresh Babu G. and Sundara Raja V., Effect of copper salt and thiourea concentrations on the formation of Cu_2ZnSnS_4 thin films by spray pyrolysis, *Phys. Status Solidi A*, **207(1)**, 149–156**(2010)**

14. Mote V.D., Purushotham Y. and Dole B.N., Williamson-Hall analysis in estimation of lattice strain in nanometer-sized ZnO particles, *J. Theor. Appl. Phys.*, **6(6)**, 1-8 **(2012)**

15. Bakr N.A., Characterization of a CdZnTe/CdTe heterostructure system prepared by Zn diffusion into a CdTe thin film, *J. Cryst. Growth,* **235(1)**, 217-223 **(2002)**

16. Daranfed W., Aida M. S., Attaf N., Bougdira J. and Rinnert H., $C_{u2}ZnSn_{S4}$ thin films deposition by ultrasonic spray pyrolysis, *J. Alloy Compd.*, **542**, 22–27**(2012)**

17. Kamoun N., Bouzouita H. and Rezig B., Fabrication and characterization of Cu_2ZnSnS_4 thin films deposited by spray pyrolysis technique, *Thin Solid Films*, **515(15)**, 5949–5952 **(2007)**

18. Saleh A.F., Structural and morphological studies of NiO thin films prepared by Rapid thermal oxidation method, *IJAIEM*, **2(1)**, 16-21 **(2013)**

19. Bakr N.A., Salman S.A. and Shano A.M., Effect of Co Doping on Structural and Optical Properties of NiO Thin Films Prepared By Chemical Spray Pyrolysis Method, *Int. lett. chem. phys. astron.*, **41**, 15-30 **(2015)**

20. Bodnar I. V. , Temperature dependence of the band gap of Cu_2ZnSnS_4 single crystals, *Semiconductors*, **49(5)**, 582-585 **(2015)**

21. Seol J.S., Lee S.Y., Lee J.C., Nam H.D. and Kim K.H., Electrical and optical properties of Cu_2ZnSnS_4 thin films prepared rf mageteon sputtering process, *Sol. Energ. Mat. Sol. Cells*, **75**, 155-162 **(2003)**

22. Tanaka T., Nagatomo T., Kawasaki D., Nishio M., Guo Q., Wakahara A., Yoshida A. and Ogawa H., Preparation of Cu_2ZnSnS_4 thin films by hybrid sputtering, *J. Phys. Chem. Solids*, **66**, 1978-1981**(2005)**

23. Wang W., Shen H., Yao H., Li J. and Jiao J., Influence of solution temperature on the properties of Cu_2ZnSnS_4 nanoparticles by ultrasound-assisted microwave irradiation, *J. Mater. Sci. Mater. Electron.*, **26(3)**, 1449-1454 **(2015)**

24. Bakr N.A., El-Hadidy H., Hammam M. and Migahed M.D., Refractive index, extinction coefficient and DC conductivity of amorphous arsenic triselenide thin film doped with silver, *Thin Solid Films*, **424**, 296–302 **(2003)**

25. Kawar S.S., Chalcogenide Thin Films Having Nanometer Grain Size for Photovoltaic Applications, *Res. J. chem. sci.*, **1(8)**, 31-35 **(2011)**

26. Solanki G.K., Gosai N.N. and Patel K.D., Structural, Optical and Dielectric Properties of Tin Selenide Nanoparticles Prepared by Aqueous Solution Method, *Res. J. chem. sci.*, **5(3)**, 1-5**(2015)**

27. Touati R., Ben Rabeh M. and Kanzari M., Structural and Optical Properties of the New Absorber Cu_2ZnSnS_4 Thin Films Grown by Vacuum Evaporation Method, *Energy Procedia*, **44**, 44 – 51 **(2014)**

28. Kahraman S., Çetinkaya S., Podlogar M., Bernik S., Çetinkara H.A. and Güder H.S., Effects of the sulfurization temperature on sol- gel processed Cu_2ZnSnS_4 thin films, *Ceram. Int.*, **39(8)**, 9285-9292 **(2013)**

29. Sarswat P.K. and Free M.L., A study of energy band gap versus temperature for Cu_2ZnSnS_4 thin films, *Physica B*, **407**, 108–111 **(2012)**

30. Al. Shammary N.F., Optical characteristics of NiO thin film on glass formed by Chemical spray pyrolysis, *J. Kufa-Phys.*, **2(1)**, 22-27 **(2010)**

31. Balu A.R., Nagarethinam V.S., Arunkumar N. and Suganya M., Nanocrystalline NiO thin films prepared by a low cost simplified spray technique using perfume atomizer, *J. Electron Devices*, **13**, 920-930 **(2012)**

32. Ahmed S.S., Hassan E.K. and G.H. Mohamed, Investigation of Optical Proper-ties of $NiO_{0.99}Cu_{0.01}$ Thin Film by Thermal Evaporation Technique, *Int. J. Adv. Res.*, **2(2)**, 633- 638 **(2014)**

33. Ezenwa I.A., Optical Analysis of Chemical bath Fabricated CuO Thin Films, *Res. J. Recent Sci.,* **1(1),** 46-50 **(2012)**

34. Okereke N. A. and Ekpunobi A. J., XRD and UV-VIS-IR Studies of Chemically-Synthesized Copper Selenide Thin Films, *Res. J. chem. sci.,* **1(6),** 64-70 **(2011)**